Published in final edited form as:
Nanotechnology. 2008 May 7; 19(18): . doi:10.1088/0957-4484/19/18/185102.

New mechanisms for non-porative ultrasound stimulation of cargo delivery to cell cytosol with targeted perfluorocarbon nanoparticles

NR Soman, **JN Marsh**, **GM Lanza**, and **SA Wickline**
Washington University School of Medicine, Consortium for Translational Research in Advanced Imaging and Nanomedicine, CTRAIN, Campus Box 8215, St Louis, MO 63110, USA

Abstract

The cell membrane constitutes a major barrier for non-endocytotic intracellular delivery of therapeutic molecules from drug delivery vehicles. Existing approaches to breaching the cell membrane include cavitational ultrasound (with microbubbles), electroporation and cell-penetrating peptides. We report the use of diagnostic ultrasound for intracellular delivery of therapeutic bulky cargo with the use of molecularly targeted liquid perfluorocarbon (PFC) nanoparticles. To demonstrate the concept, we used a lipid with a surrogate polar head group, nanogold-DPPE, incorporated into the nanoparticle lipid monolayer. Melanoma cells were incubated with nanogold particles and this was followed by insonication with continuous wave ultrasound (2.25 MHz, 5 min, 0.6 MPa). Cells not exposed to ultrasound showed gold particles partitioned only in the outer bilayer of the cell membrane with no evidence of the intracellular transit of nanogold. However, the cells exposed to ultrasound exhibited numerous nanogold-DPPE components inside the cell that appeared polarized inside intracellular vesicles demonstrating cellular uptake and trafficking. Further, ultrasound-exposed cells manifested no incorporation of calcein or the release of lactate dehydrogenase. These observations are consistent with a mechanism that suggests that ultrasound is capable of stimulating the intracellular delivery of therapeutic molecules via non-porative mechanisms. Therefore, non-cavitational adjunctive ultrasound offers a novel paradigm in intracellular cargo delivery from PFC nanoparticles.

1. Introduction

Targeted therapeutics with synthetic drug delivery vehicles (e.g. lipid or polymer-based nanoparticles) has traditionally been achieved by the endocytosis of the drug delivery vehicle followed by the release of the drug into the cytoplasm. However, lysosomal degradation and inactivation of the drug through this pathway may attenuate therapeutic benefit. Various strategies have been proposed to bypass the lysosomal pathway and achieve non-endocytotic intracellular delivery of therapeutic compounds. These include the conjugation of therapeutic cargo to a cell-penetrating peptide like TAT (Rinne *et al* 2007, Kerkis *et al* 2006, McCray *et al* 2007), electroporation (Fei *et al* 2007, Ionescu-Zanetti *et al* 2008, Deora *et al* 2007, Kusumanto *et al* 2007), and therapeutic ultrasound with microbubbles (Guzman *et al* 2001a, 2001b, Taniyama *et al* 2002, Feinstein 2004, Schlicher *et al* 2006). A common thread among these strategies is the breakdown of the cell membrane barrier through the formation of pores which allows access to the intracellular compartment.

E-mail: saw@wuphys.wustl.edu.

Ultrasound has been used in conjunction with microbubbles to drive drugs and genes into the cell by causing violent bubble cavitation and jet streaming, resulting in transient pore formation in cell membranes that may be followed by rapid annealing if the membrane damage is not severe. However, as shown both *in vitro* (Soman *et al* 2006) and *in vivo* (Miller and Quddus 2000, Wible *et al* 2002, Price *et al* 1998), cavitation also can lead to massive tissue damage and intravascular hemorrhage depending on the energies applied. An unintended consequence may be permanent damage to cells and tissues, calling into question the ultimate clinical utility of microbubbles for drug and gene delivery (Feril *et al* 2003, ter Haar 2002).

Our laboratory introduced the concept of 'contact facilitated drug delivery' with an alternative echogenic nanoparticle contrast formulation that comprised a targeted lipid-coated liquid perfluorocarbon core that was susceptible to activation by ultrasound radiation forces for augmentation of drug delivery to cells by orders of magnitude (Lanza *et al* 2002, Crowder *et al* 2005, Hughes *et al* 2005, Schmieder *et al* 2005). Drug delivery from these nanoparticles operates through a non-endocytotic energy requiring lipid-raft dependent pathway (unpublished data) whereby the transport of lipids and therapeutic molecules into cells is interlinked. This mode of lipid and drug delivery depends on the biochemical characteristics of the lipid including overall charge, size of the polar head groups, and length of fatty acid side chains (Struck and Pagano 1980, McLean and Phillipis 1981, Gummadi and Kumar 2005). However, whether this mechanism could be used to transport bulky particulates such as nanoparticles into the cytoplasm without disrupting the plasma membrane is not known. This approach could be important for targeted drug delivery to selected cells without the need for adjunctive cell-penetrating peptides such as TAT, which can compromise cell viability (Cardozo *et al* 2007).

In the present work, we report the use of ultrasound applied at mild diagnostic power levels and frequencies to achieve non-endocytotic delivery of a bulky cargo to the cytoplasm with the use of liquid perfluorocarbon nanoparticles carriers. To demonstrate the concept, we incorporated nanogold conjugated to dipalmitoyl phosphatidyl ethanolamine (nanogold-DPPE), a lipid with bulky polar head group into the lipid monolayer of the PFC nanoparticles as a cargo. In view of an earlier study that demonstrated that nanogold-DPPE would only enter cells in the presence of the pore forming antifungal compound amphotericin (Adler-Moore 1994), we sought to devise a non-cavitational ultrasound approach to achieve transcellular delivery of bulky therapeutic cargo (e.g. nanogold-DPPE) to cells without the need for membrane disruption or the use of adjunctive cell-penetrating peptides.

2. Materials and methods

2.1. Cells and cell-culture

The strategy employed was to target cancer cells with a PFC nanoparticle loaded with nanogold that also contained a specific targeting ligand to $a_v b_3$ integrins that are expressed on the cell surface. Human C-32 melanoma cells (Washington University Tissue Support Center, St Louis, MO) were grown in minimum essential medium (Earle's) supplemented with 10% bovine fetal bovine serum (Sigma, St Louis, MO). The expression of the integrin receptor $a_v b_3$ on C-32 melanoma cells was determined by flow cytometry using quantum simply cellular beads (Bangs Laboratories Inc, Fisher, IN) and was in the range of 100 000–150 000 per cell. The cells were grown on fibronectin-coated cell-culture inserts (BD Bioscience, San Jose, CA).

2.2. Synthesis of molecularly targeted perfluorocarbon nanoparticles

Perfluorocarbon nanoparticles targeted to integrin $a_v b_3$ were synthesized as described earlier (Winter *et al* 2006). Briefly, a lipid surfactant co-mixture of 99 mol% egg lecithin, 0.1 mol% peptidomimetic vitronectin antagonist specific for $a_v b_3$ integrins as shown previously (US Patent 6 322 770) conjugated to polyethylene glycol $(PEG)_{2000}$-phosphatidylethanolamine (Avanti Polar Lipids Inc, Alabaster, AL) and 0.172 mol% nanogold-dipalmitoyl-phosphatidylethanolamine (Nanoprobes Inc, Yaphank, NY) was dissolved in chloroform, evaporated under reduced pressure, dried in a 50 °C vacuum oven and dispersed into water by sonication. The suspension was combined with perfluoro-octylbromide (PFOB) (Gateway Speciality Chemicals, St Peters, MO), and distilled deionized water and continuously processed at 20 000 lbf in^{-2} for 4 min with an S110 Microfluidics emulsifier (Microfluidics, Newton, MA). This corresponded to 661 nanogold-DPPE molecules per perfluorocarbon nanoparticle. With the use of a laser light-scattering submicron particle size analyzer (Malvern Instruments, Southborough, MA), particle sizes were determined in triplicate at 37 °C to be nominally around 268 nm (range 100–800 nm).

2.3. Ultrasound apparatus

A flat single element piezoelectric transducer with a diameter of 1 cm (natural focus 1.5 cm at 2.25 MHz) was introduced in the cell-culture insert such that the distance between the cell monolayer and the bottom of the transducer was 0.5 cm (figure 1). A 100 MHz synthesized arbitrary waveform generator (Model 395, Wavetek) was used to generate sine wave pulses and the output amplified by using a RF power amplifier (Model 325, LA, Electronic Navigation Industries). Exposure to cells was carried out for approximately 5 min with continuous wave insonification at 2.25 MHz (pressure 0.6 MPa).

2.4. Transmission electron microscopy

Nanogold-DPPE perfluorocarbon nanoparticles targeted to $a_v b_3$-were incubated with C-32 melanoma cells in cell-culture inserts at 37 °C for 30 min. The cells were then exposed to continuous wave ultrasound (2.25 MHz, 0.6 MPa) for 5 min. After further incubation for 1 h at 37 °C, the cells were prefixed with 2% glutaraldehyde in 0.1 M sodium cacodylate buffer for 90 min at 4 °C. The gold nanoparticles were silver-enhanced by treating the cells with glycine (50 mM in PBC, pH 7.4), rinsing with Hepes buffer (50 mM), pH 5.8 containing sucrose (200 mM), staining with the HQ silver enhancement kit (Nanoprobes Inc, Yaphank, NY) for 3 min, and fixing with sodium thiosulfate (250 mM) in Hepes buffer (20 mM), pH 7.4 containing 200 mM sucrose. Postfixation was carried out with 0.1% osmium tetroxide in cacodylate buffer (100 mM), pH 7.4 for 30 min at 4 °C. After treatment with uranyl acetate (2% for 48 h at 37 °C), the cell-culture insert membranes were embedded in epoxy resin, thin-sectioned (60 nm) and stained with lead citrate for visualization in a Hitachi H-600 transmission electron microscope.

2.5. Confocal microscopy

C-32 melanoma cells were incubated with nanogold perfluorocarbon nanoparticles as described above. For confocal microscopy however, before exposing the cells to ultrasound, the cells were treated with 20 μg ml^{-1} rhodamine-wheat germ lectin (Vector Laboratories, Burlingame, CA) for 20 min at 4 °C to stain the plasma membrane. Calcein (Sigma, St Louis, MO), a green-fluorescent marker that is impermeant to viable cells and independent of pH between 6.5 and 12, was introduced in the media at 100 μM. After exposing the cells to ultrasound, the cells were washed extensively and fixed with 4% paraformaldehyde for 10 min at room temperature prior to visualization with a Zeiss 510 confocal microscope.

2.6. Lactate dehydrogenase release assay

Lactate dehydrogenase is an intracellular enzyme that is released from the cells after membrane damage. The LDH release assay was performed according to manufacturer's instructions (BioVision Inc, Mountain View, CA). Briefly, C-32 melanoma cells were exposed to ultrasound (as described above) in the absence or presence of $a_v b_3$-integrin targeted perfluorocarbon nanoparticles or 0.25% v/v Definity® (Bristol Myers Squibb Medical Imaging, MA). The supernatant was then assayed for the presence of LDH. Cells treated with 1% triton-X were used as a positive control.

3. Results

3.1. Nontreated cell response

Electron micrographic images of silver-enhanced nanogold perfluorocarbon nanoparticles interacting with C-32 melanoma cells are shown in figure 2. At a very early stage of interaction (figures 2(A) and (B)), intact perfluorocarbon nanoparticles were observed binding to the cell membrane. Subsequently, at a later stage (2 h), the nanogold-DPPE from the nanoparticle was observed in the outer cell layer (figures 2(C) and (D)). Similar patterns were apparent at 12 h (data not shown). This confirms that although the nanoparticle fuses with the cell membrane as anticipated from prior work (Crowder *et al* 2005), nanogold-DPPE is not internalized into the cell under simple incubation conditions thereby reinforcing the findings of Adler-Moore (1994).

3.2. Ultrasound treated cell response

Figure 3 shows C-32 melanoma cells interacting with perfluorocarbon nanoparticles 2 h after exposure to 5 min of continuous wave ultrasound (2.25 MHz). Nanogold now can be seen to be internalized in the cell beyond the cell membrane with no apparent damage to the cell. The nanogold material appears to traffic in the cytoplasm within uni-vesicular (figures 3(A)–(C)) or multi-vesicular bodies (figure 3(D)).

3.3. Cell viability

Calcein is an extracellular marker that does not enter intact viable cells. When C-32 melanoma cells were exposed to ultrasound in the presence or absence of nanogold perfluorocarbon nanoparticles, calcein could not be detected in the cell (figure 4(A)). As a positive control, the cells were treated with 0.1% triton-X 100 (Sigma, St Louis, MO), a chemical that is known to permeabilize the cell membrane. For the LDH assay too, cells treated with 0.1% Triton-X 100 were considered as positive control (100% release). The LDH release from cells not treated with ultrasound or PFC nanoparticles was 8.9 ± 4.2%. No significant difference in LDH release was observed after C-32 melanoma cells were exposed to ultrasound in the presence (12.1 ± 4.6%) or absence (11.5 ± 5.4%) of $a_v b_3$-targeted perfluorocarbon nanoparticles (figure 4(B)). Under similar conditions, cells exposed to ultrasound in the presence of Definity® showed a significant difference ($p < 0.05$, t-test) in LDH release (24.7 ± 6.4%).

4. Discussion

Targeted pharmaceutical delivery vehicles typically depend on cellular endocytosis to achieve intracellular delivery of drugs and genes. However, endocytosis of carriers is size dependent and cell-type dependent. For example, the binding of anti-PECAM immunoconjugates to human endothelial cells leads to endocytosis only if their size is less than 300 nm (Wiewrodt *et al* 2002). Even after endocytosis of the carrier is achieved, the degradation of the active therapeutic molecule in the endosomal–lysosomal pathway may compromise overall efficacy. Existing strategies for bypassing endocytotic pathways to gain

direct cytosolic access require breaching the cell membrane barrier (e.g. cell-penetrating peptides, electroporation, ultrasound with microbubbles), which may damage or kill the targeted cell (Price *et al* 1998, Miller and Quddus 2000, Cardozo *et al* 2007).

Targeted lipid-coated perfluorocarbon nanoparticles serve as a effective synthetic delivery vehicle for therapeutic molecules that typically bypasses endocytosis. The delivery of drugs and lipids from these nanoparticles to targeted cells likely occurs through contact-mediated vesicle-cell fusion whereby the lipid monolayer of the nanoparticle fuses with the cell membrane allowing the intermixing of nanoparticle lipids with the cell membrane lipids due to lateral diffusion. Further transport into the cell is dependent on lipid flip-flop from the outer to inner membrane and lipid trafficking via caveolae and lipid rafts. The process is energy requiring, as is also the case for endocytosis, and can be inhibited at cold temperatures or by ATP depletion (Partlow K, Lanza G, Wickline S, unpublished data).

An important consideration for such lipid-based membrane-fusional drug delivery approaches is the fact that lipid transport can be affected by a wide variety of factors, chief being the size of the polar head groups and the lengths of the fatty acid side chains (Gummadi and Kumar 2005). Early studies on fusion of lipid vesicles indicated that lipids conjugated to different fluorophores like rhodamine or fluorescein exhibit different diffusion coefficients (McLean and Phillipis 1981). Further, the size of the lipid also affects it's cellular trafficking. For example, as shown by Adler-Moore (1994), lipids conjugated to nanogold do not internalize by themselves but require additional means (e.g., pores) to gain cellular entry. The present studies of transport of bulky polar head group lipids (nanogold-DPPE) demonstrate that nanogold-DPPE was confined to the cell membrane after fusion and lipid mixing (figure 2), but were not otherwise capable of unassisted intracellular transport. As shown earlier (Adler-Moore 1994), transport of the DPPE conjugated to a bulky nanogold (diameter 1.4 nm) was inhibited, likely because it is unable to flip to the inner membrane leaflet.

We have shown previously that clinical ultrasound energy delivered in vitro to cells in the presence of untargeted or targeted PFC nanoparticles can enhance their interaction with cells thereby dramatically increasing lipid delivery many fold (Crowder *et al* 2005). Further, the uptake of lipidic molecules was far greater from a_vb_3-targeted PFC nanoparticles than non-targeted ones. We have also shown that ultrasound (0.5 and 0.2 MPa) used with microbubbles (Definity®) can cause focal disruptions in the vasculature but when used with PFC nanoparticles do not cause any damage to endothelial cell integrity (Soman *et al* 2006). Our goal in this study was to employ similar ultrasound parameters and study its effect on the transport of bulky therapeutic cargo (e.g. nanogold-DPPE) from targeted PFC nanoparticles. When C-32 melanoma cells were exposed to continuous wave ultrasound (2.25 MHz for 5 min), nanogold-DPPE was observed inside intracellular vesicles. Ultrasound augmentation of lipid-particulate transport under quite mild conditions was therefore able to overcome the biophysical barriers to lipid trafficking.

Ultrasound in presence of microbubbles has been used to drive drugs and genes into the cell by formation of transient membrane pores as a direct result of cavitation (Feinstein 2004). Recently, low-frequency ultrasound (24 kHz) has been shown to cause transient pores (analogous to wound healing) without the use of cavitational agents (Schlicher *et al* 2006). However these effects may under certain conditions compromise cell viability (ter Haar 2002) and cause release of LDH as shown in figure 4(B). When C-32 melanoma cells were exposed to continuous ultrasound in the presence or absence of nanogold perfluorocarbon nanoparticles, calcein (an extracellular marker) was not internalized into the cell as demonstrated in the confocal micrographs (figure 4(A)) and no release of intracellular lactate dehydrogenase was observed. These data further indicate that the internalization of

nanogold-DPPE is not due to transient discontinuities in the cell membrane, but more likely is related to the specific binding and close apposition of the nanoparticles to the targeted cell membrane.

Previous studies have shown that the cell adhesion molecules such as integrins (e.g., $a_v b_3$) respond to mechanical stimuli and alter biochemical and gene expression. The integrins thus form the interface for mechano-biological transduction (Ingber 2006). Ultrasound traveling compressional waves induce a temporal-averaged force on the medium (i.e., radiation force) that has been implicated in bone repair (Wang *et al* 2001), tactile response (Dalecki *et al* 1995) and auditory response (Tsirulkinov *et al* 1988). When such a force acts on a PFC nanoparticle, it is clear that it can augment the interaction between the PFC nanoparticle and the cells, and the same applies to these solid gold nanoparticles which otherwise would not penetrate the cell membrane. Ultrasound radiation forces enhance this interaction and lead to the internalization of therapeutic cargo. The mechanisms responsible for this ultrasound transport effect could be multiple, but clearly are not associated with pore formation (sonoporation), membrane disruption, or cavitation. For example, ultrasound could supply the necessary energy to augment lipid flipping, which typically is provided by ATP-requiring flippases, followed by lipid-raft formation and transport (Holthius and Levine 2005, Wenk 2005). A variety of other possibilities exist, but it is interesting to note that once internalized, the lipid–nanogold particles traffic to intracellular vesicles as part of their membrane components (figure 3). Further work will be required to characterize molecular mechanisms responsible and to assess the ultimate disposition of these types of complexes.

In conclusion, our goal was to demonstrate a unique approach to ultrasound-mediated therapeutic cargo delivery to cell cytosol by PFC nanoparticles without deleterious pore formation. Our study shows that non-cavitational ultrasound used in conjunction with liquid perfluorocarbon nanoparticles can induce the uptake and internalization of lipids (and possibly other therapeutic molecules) that would not otherwise be delivered to the cytosol of target cells due to biophysical constraints. Fluorescent microscopy and LDH assay implies that the mechanism of interaction of ultrasound and targeted perfluorocarbon nanoparticles in influencing lipid delivery is not through the formation of pores or transient discontinuities in the cell membrane. The enhanced drug delivery might however be influenced by specific targeting of nanoparticles which when acted upon by ultrasound radiation forces gain sufficient energy to overcome the biophysical barriers to lipid flip-flop or other energy requiring mechanisms. The implications for clinical augmentation of lipophilic drug delivery with conventional ultrasound imaging devices are pertinent to pharmacodynamic profiling.

Acknowledgments

This work was supported in part by the US National Institutes of Health (Grant HL-42590 and HL-59865) to S A Wickline and the American Heart Association Predoctoral fellowship (0515446Z) to N R Soman.

References

Adler-Moore J. AmBisome targeting to fungal infections. Bone Marrow Transplant. 1994; 14:S3–7. Review. [PubMed: 7703928]

Cardozo AK, et al. Cell-permeable peptides induce dose-and length-dependent cytotoxic effects. Biochim Biophys Acta. 2007; 1768:2222–34. [PubMed: 17626783]

Crowder KC, Hughes MS, Marsh JN, Barbeiri AM, Fuhrhop RW, Lanza GM, Wickline SA. Sonic activation of molecularly-targeted nanoparticles accelerates transmembrane lipid delivery to cancer cells through contact-mediated mechanisms: implications for enhanced local drug delivery. Ultrasound Med Biol. 2005; 31:693–700. [PubMed: 15866419]

Dalecki D, Child SZ, Raeman CH, Carstensen EL. Tactile perception of ultrasound. J Acoust Soc Am. 1995; 97:3165–70. [PubMed: 7759656]

Deora AA, Diaz F, Schreiner R, Rodriguez-Boulan E. Efficient electroporation of DNA and protein into confluent and differentiated epithelial cells in culture. Traffic. 2007; 8:1304–12. [PubMed: 17662027]

Fei Z, Wang S, Xie Y, Henslee BE, Koh CG, Lee LJ. Gene transfection of mammalian cells using membrane sandwich electroporation. Anal Chem. 2007; 79:5719–22. [PubMed: 17600386]

Feinstein SB. The powerful microbubble: from bench to bedside, from intravascular indicator to therapeutic delivery system, and beyond. Am J Physiol Heart Circ Physiol. 2004; 287:H450–7. [PubMed: 15277188]

Feril LB Jr, Kondo T, Zhao QL, Ogawa R, Tachibana K, Kudo N, Fujimoto S, Nakamura S. Enhancement of ultrasound-induced apoptosis and cell lysis by echo-contrast agents. Ultrasound Med Biol. 2003; 29:331–7. [PubMed: 12659921]

Gummadi SN, Kumar KS. The mystery of phospholipid flip-flop in biogenic membranes. Cell Miol Biol Lett. 2005; 10:101–21.

Guzman HR, Nguyen DX, Khan S, Prausnitz MR. Ultrasound-mediated disruption of cell membranes I. Quantification of molecular uptake and cell viability. J Acoust Soc Am. 2001a; 110:588–96. [PubMed: 11508983]

Guzman HR, Nguyen DX, Khan S, Prausnitz MR. Ultrasound-mediated disruption of cell membranes II. Heterogenous effects on cells. J Acoust Soc Am. 2001b; 110:597–606. [PubMed: 11508985]

Holthius JC, Levine TP. Lipid traffic: floppy drives and a superhighway. Nat Rev Mol Cell Biol. 2005; 6:209–20. [PubMed: 15738987]

Hughes MS, Marsh JN, Hall CS, Fuhrhop RW, Lacy EK, Lanza GM, Wickline SA. Acoustic characterization in whole blood and plasma of site-targeted nanoparticle ultrasound contrast agent for molecular imaging. J Acoust Soc Am. 2005; 117:964–72. [PubMed: 15759715]

Ingber DE. Cellular mechanotransduction: putting all the pieces together again. FASEB J. 2006; 20:811–27. [PubMed: 16675838]

Ionescu-Zanetti C, Blatz A, Khine M. Electrophoresis-assisted single-cell electroporation for efficient intracellular delivery. Biomed Microdevices. 2008; 10:113–6. [PubMed: 17828458]

Kerkis A, Hayashi MA, Yamane T, Kerkis I. Properties of cell penetrating peptides (CPPs). IUBMB Life. 2006; 58:7–13. Review. [PubMed: 16540427]

Kusumanto YH, Mulder NH, Dam WA, Losen MH, Meijer C, Hospers GA. Improvement of in vivo transfer of plasmid DNA in muscle: comparison of electroporation versus ultrasound. Drug Deliv. 2007; 14:273–7. [PubMed: 17613014]

Lanza GM, Yu X, Winter PM, Abendschein DR, Karukstis K, Scott MJ, Chinen LK, Fuhrhop RW, Scherrer DE, Wickline SA. Targeted antiproliferative drug delivery to vascular smooth muscle cells with a magnetic resonance imaging nanoparticle contrast agent: implications for the rational therapy of restenosis. Circulation. 2002; 106:2842–7. [PubMed: 12451012]

McCray AN, Ugen KE, Heller R. Enhancement of anti-melanoma activity of a plasmid expressing HIV Vpr delivered through in vivo electroporation. Cancer Bio Ther. 2007; 6:1269–75. [PubMed: 17700061]

McLean LR, Phillipis MC. Mechanism of cholesterol and phosphatidylcholine exchange or transfer between unilamellar vesicles. Biochemistry. 1981; 20:2893–900. [PubMed: 7195733]

Miller DL, Quddus J. Diagnostic ultrasound activation of contrast agent gas bodies induces capillary rupture in mice. Proc Natl Acad Sci USA. 2000; 97:10179–84. [PubMed: 10954753]

Price RJ, Skyba DM, Kaul S, Skalak TC. Delivery of colloidal particles and red blood cells to tissue through microvessel ruptures created by targeted microbubble destruction with ultrasound. Circulation. 1998; 98:1264–7. [PubMed: 9751673]

Rinne J, Albarran B, Jylhävä J, Ihalainen T, Kankaanpää P, Hytönen V, Stayton P, Kulomaa M, Vihinen-Ranta M. Internalization of novel non-viral vector TAT-streptavidin into human cells. BMC Biotechnol. 2007; 7:1. [PubMed: 17199888]

Schlicher RK, Radhakrishna H, Tolentino TP, Apkarian RP, Zarnitsyn V, Prausnitz MR. Mechanism of intracellular delivery by acoustic cavitation. Ultrasound Med Biol. 2006; 32:915–24. [PubMed: 16785013]

Schmieder AH, et al. Molecular MR imaging of melanoma angiogenesis with alphavbeta3-targeted paramagnetic nanoparticles. Magn Reson Med. 2005; 53:621–7. [PubMed: 15723405]

Soman NR, Marsh JN, Hughes MS, Lanza GM, Wickline SA. Acoustic activation of targeted liquid perfluorocarbon nanoparticles does not compromise endothelial integrity. IEEE Trans Nanobiosci. 2006; 5:69–75.

Struck DK, Pagano RE. Insertion of fluorescent phospholipids into the plasma membrane of a mammalian cell. J Biol Chem. 1980; 255:5404–10. [PubMed: 7372642]

Taniyama Y, Tachibana K, Hiraoka K, Namba T, Yamasaki K, Hashiya N, Aoki M, Ogihara T, Yasufumi K, Morishita R. Local delivery of plasmid DNA into rat carotid artery using ultrasound. Circulation. 2002; 105:1233–9. [PubMed: 11889019]

ter Haar GR. Ultrasonic contrast agents: safety considerations reviewed. Eur J Radiol. 2002; 41:217–21. [PubMed: 11861096]

Tsirulkinov EM, Vartanyan IA, Gersuni GV, Rosenblyum AS, Pudov VI, Gavrilov LR. Use of amplitude-modulated focused ultrasound for diagnosis for hearing disorders. Ultrasound Med Biol. 1988; 14:277–85. [PubMed: 3046092]

Wang C, Chen H, Chen C, Yang K. Treatment of nonunions of long bone fractures with shock waves. Clin Orthop. 2001; 387:95–101. [PubMed: 11400901]

Wenk MR. The emerging field of lipidomics. Nature. 2005; 4:594–610.

Wible JH Jr, Galen KP, Wojdyla JK, Hughes MS, Klibanov AL, Brandenburger GH. Microbubbles induce renal hemorrhage when exposed to diagnostic ultrasound in anesthetized rats. Ultrasound Med Biol. 2002; 28:1535–46. [PubMed: 12498949]

Wiewrodt R, Thomas AP, Cipelletti L, Christofidou-Solomidou M, Weitz DA, Feinstein SI, Schaffer D, Albelda SM, Koval M, Muzykantov VR. Size-dependent intracellular immunotargeting of therapeutic cargoes into endothelial cells. Blood. 2002; 99:912–22. [PubMed: 11806994]

Winter PM, et al. Endothelial alpha(v)beta3 integrin-targeted fumagillin nanoparticles inhibit angiogenesis in atherosclerosis. Arterioscler Thromb Vasc Biol. 2006; 26:2103–9. [PubMed: 16825592]

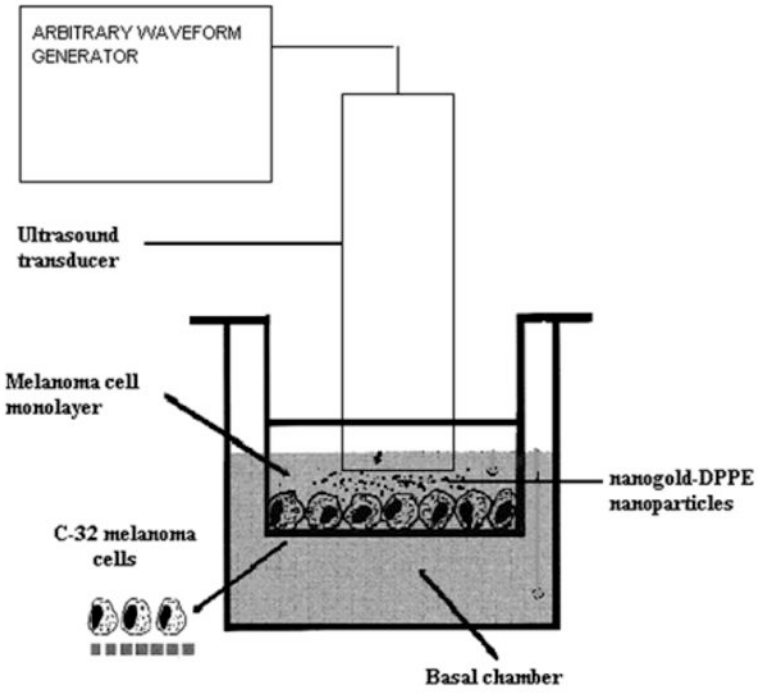

Figure 1.

In vitro sonication setup showing single element piezoelectric transducer introduced in a cell-culture insert with nanogold-DPPE perfluorocarbon nanoparticles bound to a monolayer of C-32 melanoma cells.

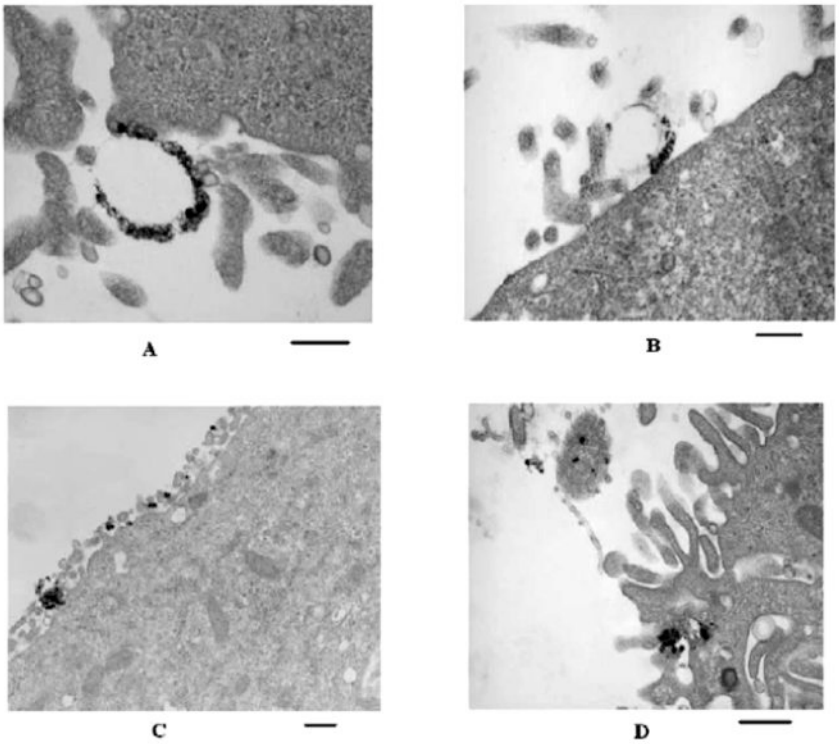

Figure 2.

A lipid with a bulky polar head group (nanogold-DPPE) is not internalized into the cell when delivered from a_vb_3 targeted perfluorocarbon nanoparticles in the absence of ultrasound. Transmission electron micrographs showing the interaction of silver-enhanced nanogold-DPPE perfluorocarbon nanoparticles with C-32 melanoma cells in the absence of ultrasound. The nanogold-DPPE nanoparticles can be seen bound to the cell membrane ((A) and (B)) after 1 h of incubation at 37 °C while after 3 h nanogold-DPPE is seen to have moved to the cell membrane. No internalization of nanogold-DPPE was seen even after 12 h of incubation. The bar corresponds to 400 nm.

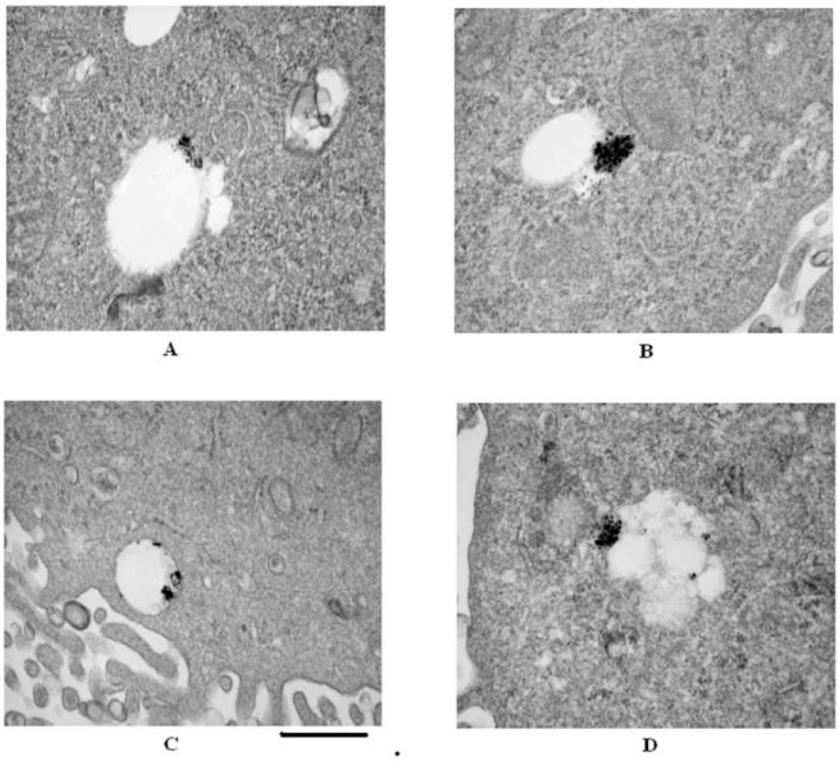

Figure 3.
Ultrasound triggers internalization of nanogold-DPPE delivered from $a_v b_3$-targeted perfluorocarbon nanoparticles. Transmission electron micrographs of silver-enhanced nanogold-DPPE perfluorocarbon nanoparticles interacting with C-32 melanoma cells after exposure to continuous wave ultrasound (2.25 MHz, 5 min). Nanogold-DPPE can be seen polarized inside intracellular vesicles. The bar corresponds to 400 nm.

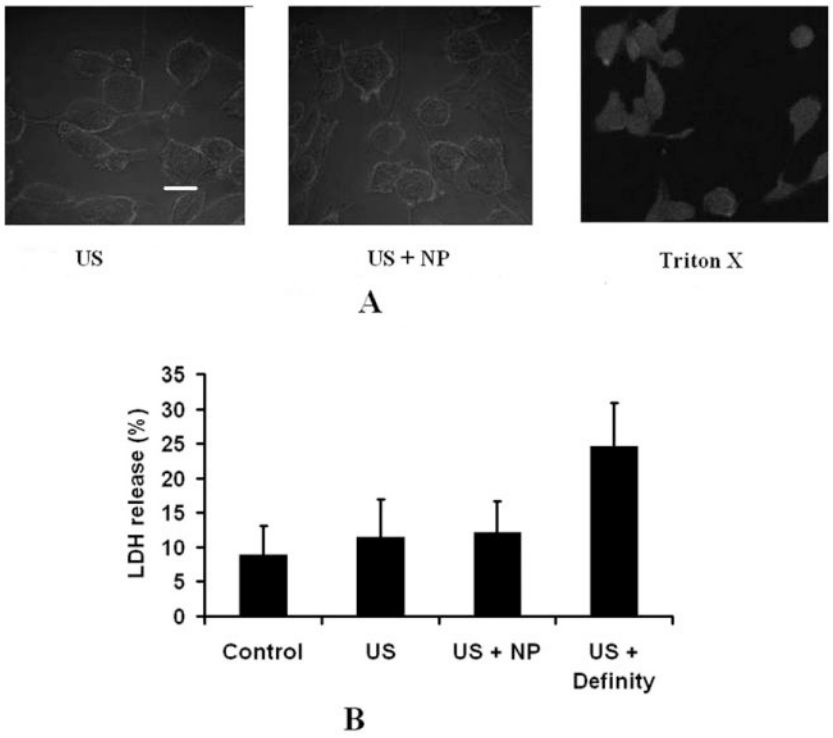

Figure 4.

Ultrasound in conjunction with liquid perfluorocarbon nanoparticles does not cause cell membrane damage. (A) Confocal micrographs of C-32 melanoma cells exposed to continuous wave ultrasound (2.25 MHz for 5 min) in the presence or absence of perfluorocarbon nanoparticles. Cells treated with 0.1% triton-X are shown as positive control (red: rhodamine-wheat germ lectin, green: calcein); the bar indicates 20 μm. (B) Release of lactate dehydrogenase (LDH) from C-32 melanoma cells treated with either Definity® or $a_v b_3$-targeted nanoparticles and ultrasound. Cells treated with triton-X were considered as 100% release. US: ultrasound, NP: nanoparticles.